



The Use of Explicit Filters in Large Eddy Simulation

T. S. LUND

Department of Mechanical and Aerospace Engineering
University of Texas at Arlington
Box 19018, Arlington, TX 76019-0018, U.S.A.

Abstract—Explicit filtering is considered as a means of controlling the numerical errors that result when finite-difference methods are used in large eddy simulation (LES). The notion that the finite-difference expressions themselves act as an effective filter is shown to be false for three-dimensional simulations performed on nonuniform meshes. For consistency, the nonlinear terms in the Navier-Stokes equations should be filtered explicitly at each time step in order to insure that the spectral content of the solution remains fixed at the desired filter level. The explicit filtering operation allows a separation between the filter size and the mesh spacing and can be used to control the impact of the numerical errors. Numerical tests of the explicit filtering approach in turbulent channel flow are used to investigate the effectiveness of the explicit filtering approach and to assess its associated cost. Explicit filtering is shown to improve the computed results, but this improvement comes at a rather high computational cost. The explicitly-filtered approach is also compared with straightforward mesh refinement as an alternative means of improving the computed results. Mesh refinement is also seen to increase the accuracy of the simulation but some traces of numerical error appear to persist in the solution. © 2003 Elsevier Ltd. All rights reserved.

Keywords—Large eddy simulation, Filtering, Subgrid-scale modelling, Turbulence, Numerical simulation.

1. INTRODUCTION

The equations for large eddy simulation (LES) are derived formally by applying a low pass-filter to the Navier-Stokes equations. The filter width, as well as the details of the filter shape, are free parameteres in LES and these can be used to advantage in order to control the effective resolution of the simulation as well as to limit the errors associated with the numerical solution procedure.

In spite of the importance and potential utility of the filtering operation, the vast majority of large eddy simulations performed to date using finite-difference approximations have made little or no use of an explicit filtering of the Navier-Stokes equations in the solution procedure. The nearly universal approach is to simply write down the filtered Navier-Stokes equations together with an assumed model for the subgrid-scale stresses and then apply the desired spatial discretization to this “filtered” system. Although it is rarely mentioned, what one is doing by adopting this procedure is to imagine that the finite support of the computational mesh together with the low-pass characteristics of the discrete differentiating operators act as an effective filter. One then directly associates the computed velocity field with the filtered velocity. This procedure will be

This work was initiated when the author was in residence at the Center for Turbulence Research. Computer time was supplied by the NASA Ames Research Center and is gratefully acknowledged.

referred to as implicit filtering since an explicit filtering operation never appears in the solution procedure.

Although the technique of implicit filtering has been used extensively, there are several compelling reasons to adopt a more systematic approach. Foremost of these is the issue of consistency. While it is true, that discrete derivative operators have a low-pass filtering effect, we will show that the associated filter acts only in the single spatial direction in which the derivative is taken. This fact implies that each term in the Navier-Stokes equations is acted on by a distinct one-dimensional filter, and thus, there is no way to derive the discrete equations through the uniform application of a single three-dimensional filter. Considering this ambiguity in the definition of the filter, it is difficult to make meaningful comparisons of LES results with filtered experimental or direct numerical simulation (DNS) data.

A further inconsistency associated with implicit filtering arises from its inability to control the frequency content of the advective terms. In deriving the filtered equations, one replaces $\overline{u_i u_j}$ with $\overline{u_i} \overline{u_j} + \tau_{ij}$. Prior to this replacement, each term in the filtered Navier-Stokes equations had its frequency content limited to the bar level. Following the replacement, this condition is removed from the advective terms and they are free to generate higher frequencies due to nonlinear interactions. Although a properly-constructed subgrid-scale model could potentially offset this effect, such a consideration rarely appears as a modelling constraint.¹ In practice, the inconsistently-generated high frequencies alias back to the resolved portion of the spectrum and interfere with the dynamics of the turbulence over a broad scale range.

A final significant drawback of the implicit filtering approach is the inability to control numerical error. Nearly all discrete derivative operators become rather inaccurate for high frequency solution components and this error interferes with the dynamics of the smallest resolved eddies. By definition, these eddies are important in LES and one cannot overlook the interaction of the phase errors with the turbulence cascade mechanism for the smallest computed scales. This error can be particularly harmful when the dynamic model [1,2] is used since it relies entirely on information contained in the smallest resolved scales.

The difficulties associated with the implicit filtering approach can be alleviated by performing an explicit filtering operation as an integral part of the solution process. In this approach, the advective terms are recast, as $\overline{\overline{u_i} \overline{u_j}} + \tau'_{ij}$, where the filtering of the nonlinear product is performed explicitly. This operation returns the frequency content of the advective terms to the bar level, and thus, restores a consistent level of spectral content to each term in the numerical solution of the filtered Navier-Stokes equations. Furthermore, if the filter scale is chosen to be larger than the mesh spacing, it is possible to permanently damp the small-scale motions that are admitted by the mesh, but not accurately represented by the discrete differencing operators. This feature can be used to remove the bulk of the truncation error that otherwise contaminate the frequencies near the mesh cutoff. Numerical errors can thus be separated from the physical processes and, if the filter width is held fixed as the mesh is refined, the velocity field ultimately converges to the true solution of the filtered Navier-Stokes equations. Finally, the filter is defined unambiguously in the explicitly-filtered approach, and thus, comparisons with experimental or DNS data is straightforward.

Given the advantages of explicit filtering, it may seem puzzling that it is used so rarely. There are several good reasons for this state of affairs, and perhaps the most compelling of these is the prior absence of filter operators that commute with finite-difference operators on nonuniform meshes. Without commuting operators, the act of filtering alters the Navier-Stokes equations through the addition of 'communication error terms' [3]. Although one could in principle include the communication error terms in the solution procedure, this would add a significant complication and raise further questions regarding the required additional numerical approximations.

¹As shown later, scale similarity models as well as those that compute the Leonard term explicitly make some headway in this direction.

The unresolved communication issue stood as a practical deterrent to explicit filtering for nearly 25 years.

Recently, several filtering schemes have been developed that commute with finite-difference operators up to a specified order of accuracy on nonuniform meshes [3–5]. These new filter operators pave the way for the consistent use of explicit filtering in LES. The class of filters presented by Vasilyev *et al.* [5] take the particularly simple form of local spatial averages and can be made to commute with finite-derivative operators of arbitrary order.

A second, more practical consideration, in the use of explicit filtering is the associated numerical cost. By removing the high-frequency solution components, explicit filtering reduces the effective resolution of the simulation compared with the dynamic range supported by the mesh. Thus, it is necessary to use a mesh that is somewhat finer than the smallest eddy that one hopes to resolve. In 3-D this can amount to a large overhead since the mesh must be refined in each direction independently. A filter width ratio of 1.5 increases the cost of the simulation by a factor of $1.5^3 = 3.4$, whereas a filter ratio of 3 increases the cost by a factor of $3^3 = 27$! This significant increase is alarming but can at least be tolerated on present day supercomputers.

The potentially high cost of explicit filtering raises several interesting questions regarding its utility. Specifically, how rapidly does the solution improve as the filter width ratio is increased? What price should one be willing to pay for increased numerical fidelity? Why not take advantage of the increased resolution and simply perform an unfiltered simulation on the expanded mesh? The last point is particularly interesting since it could form the basis of a philosophical debate. A purist may take the point of view that one should be mindful of consistency and should strive to minimize numerical error whenever possible and, would thus, adopt the explicitly filtered approach. A more practically minded person may be satisfied with the fact that the numerical errors in an implicitly filtered simulation on the expanded mesh are concentrated at very small scales which may be dynamically unimportant from a LES perspective. Both approaches share the same computational overhead and have identical numerical fidelity for length scales larger than the filter width. In the explicitly-filtered case, however, turbulent motions smaller than the filter width are effectively removed from the simulation and their effect is delegated to the subgrid-scale model. In performing implicitly-filtered simulations on the expanded mesh, one is allowing the error-prone length scales smaller than the filter width to remain in the simulation in the hopes that their dynamic effect on the large scales is small. In order, to draw an analogy with the explicitly-filtered case, one can think of these small scale motions (together with the small contribution from the subgrid-scale model applied to the scale of the mesh spacing) as an effective subgrid-scale model for the portion of the velocity field up to the assumed filter width. In spite of the contamination by numerical error, it is certainly possible that the directly simulated small scale motions form a subgrid-scale model that is superior to the simple algebraic models that are commonly used.

The purpose of this paper is twofold:

- (1) to develop the framework for explicit filtering in LES, and
- (2) to explore the effectiveness of the explicit filtering approach for LES of turbulent channel flow.

2. EXPLICIT FILTERING PROCEDURE

Application of a commuting filter to the Navier-Stokes equations leads to

$$\frac{\partial \bar{u}_i}{\partial x_i} = 0, \quad (1)$$

$$\frac{\partial \bar{u}_i}{\partial t} + \frac{\partial \bar{u}_i \bar{u}_j}{\partial x_j} = -\frac{\partial \bar{p}}{\partial x_i} + \frac{1}{Re} \frac{\partial^2 \bar{u}_i}{\partial x_j \partial x_j}, \quad (2)$$

where p is the thermodynamic pressure divided by the density. The correlation $\bar{u}_i \bar{u}_j$ is unknown in LES and is typically treated by computing the product of the filtered velocities and modelling

the remainder, i.e.,

$$\overline{u_i u_j} = \overline{u_i} \overline{u_j} + \underbrace{(\overline{u_i u_j} - \overline{u_i} \overline{u_j})}_{\tau_{ij}}. \quad (3)$$

If this decomposition together with a model for τ_{ij} is substituted into the filtered momentum equation, a closed equation for $\overline{u_i}$ is obtained. It would then appear that the filtered Navier-Stokes equations could be advanced in time from an initial $\overline{u_i}$ field without ever performing a filtering operation in the solution process. While this observation seems a bit unsettling, it is often argued that the wavenumber-dependent characteristic of finite-differencing errors act as an effective 'implicit filter'. This argument is based on the following equivalence between a finite difference and the exact derivative of a filtered variable [6]

$$\left. \frac{\delta u}{\delta x} \right|_i = \frac{u_{i+1} - u_{i-1}}{2\Delta x} = \frac{d}{dx} \left[\frac{1}{2\Delta x} \int_{x_{i-1}}^{x_{i+1}} u dx \right] = \left. \frac{d\overline{u}}{dx} \right|_i. \quad (4)$$

While this equivalence is undoubtedly genuine, there are two significant problems with extending the above observation to filtering as it applies to the solution of the LES equations. First, the equivalence requires a connection between the exact derivative of the filtered variable and the finite difference of the *unfiltered variable*. Thus, a strict application of this law to the filtered Navier-Stokes equations would require that the original filterings be removed when the finite-difference approximation is made. In order, to avoid this problem, one can consider applying a second filter to the Navier-Stokes equations and allow this one to be removed when the finite differences are taken. As we shall see, this argument cannot be made rigorous either due to the second complication that has to do with the multidimensionality associated with the Navier-Stokes equations. The filter used to derive the LES equations must be a three-dimensional operation that represents averaging the velocity field over a small volume in space. The filter implied by the finite-difference operator, on the other hand, represents an average in a single coordinate direction. Thus, each term in the LES equations is effectively acted on by a different one-dimensional filter when finite differences are used. In particular, the actual equation being solved is

$$\begin{aligned} \frac{\partial \overline{u_i}}{\partial t} + \frac{\partial \widetilde{\overline{u_i} \overline{u_1}}^{x_1}}{\partial x_1} + \frac{\partial \widetilde{\overline{u_i} \overline{u_2}}^{x_2}}{\partial x_2} + \frac{\partial \widetilde{\overline{u_i} \overline{u_3}}^{x_3}}{\partial x_3} = & - \frac{\partial \widetilde{\overline{p}}^{x_i}}{\partial x_i} - \frac{\partial \widetilde{\overline{\tau}_{i1}}^{x_1}}{\partial x_1} - \frac{\partial \widetilde{\overline{\tau}_{i2}}^{x_2}}{\partial x_2} - \frac{\partial \widetilde{\overline{\tau}_{i3}}^{x_3}}{\partial x_3} \\ & + \frac{1}{Re} \left[\frac{\partial^2 \widetilde{\overline{u_i}}^{x_1}}{\partial^2 x_1} + \frac{\partial^2 \widetilde{\overline{u_i}}^{x_2}}{\partial^2 x_2} + \frac{\partial^2 \widetilde{\overline{u_i}}^{x_3}}{\partial^2 x_3} \right], \end{aligned} \quad (5)$$

where $\widetilde{(\)}^{x_i}$ and $\widehat{(\)}^{x_i}$ are the effective one-dimensional filters associated with the first- and second-difference approximations, respectively. It should be clear that the above equation cannot be derived from the Navier-Stokes equations since the various effective filters are not distributed uniformly. We conclude that although there is an inherent filtering operation associated with finite-difference approximations, their use does not lead to a well-defined effective three-dimensional filter.

With the issues associated with finite differences aside, there is another difficulty associated with the use of the decomposition given in equation (3). The problem with this formulation is that the nonlinear product $\overline{u_i} \overline{u_j}$ generates frequencies beyond the characteristic frequency that defines $\overline{u_i}$. These high frequencies alias back as resolved ones, and therefore, act as fictitious stresses. In principle, the subgrid-scale model, τ_{ij} , could exactly cancel this effect, but this has rarely appeared as a subgrid-scale modelling constraint. The obvious way to control the frequency content of the nonlinear terms is to filter them. This strategy would result in the following alternative decomposition:

$$\overline{u_i u_j} = \overline{\overline{u_i} \overline{u_j}} + \underbrace{(\overline{u_i u_j} - \overline{\overline{u_i} \overline{u_j}})}_{\tau'_{ij}}. \quad (6)$$

If this relation together with a subgrid-scale model for τ'_{ij} is substituted into equation (2), one again obtains a closed equation for \bar{u}_i , but this time with an additional *explicit filtering* operation applied to the nonlinear term. This procedure is similar to approaches where the Leonard term is computed explicitly and a model (τ'_{ij}) is used only for the cross and Reynolds stresses. The important difference here is that the filter width is taken to be larger than the mesh spacing and one uses a properly-defined commuting filter.

It is now apparent that the implicit filtering implied by the finite-difference operators shown in equation (5) is vaguely similar to the explicitly-filtered approach, although the one-dimensional filterings are not nearly as effective at controlling the frequency content of the solution.

While the decomposition of equation (6) has several advantageous properties from the point of view of explicit filtering, there is one significant side effect that should be mentioned. It can be shown that if equation (6) is substituted into equation (2), the resulting equation is, in general, not Galilean invariant. The residual takes the form $c_j \frac{d(\bar{u}_i - \bar{u}_i)}{dx_j}$, where c_j is the uniform translation velocity. The error is seen to be proportional to the difference between the singly and doubly filtered velocity. This difference will be zero for a Fourier cutoff filter, but will not vanish in the general case. The spectral content of the error is proportional to $G(k)(1 - G(K))$ where $G(k)$ is the filter transfer function. This fact implies that error is generated only in the wavenumber band where $G(k)$ differs significantly from 0 or 1. It is also clear that the error is maximized at 25%. Thus, it is possible to minimize the error by constructing the explicit filter to be as close as possible to a Fourier cutoff. It is also possible to eliminate the Galilean invariance error all together by switching to yet another alternative decomposition for the advective terms. This step amounts to adding a scale-similarity like term to the filtered Navier-Stokes equations. The difficulty in this approach is that the scale-similarity model can generate frequencies above the filter cutoff, and thus, weakens the explicit filtering approach. At the present time, it appears best to continue with equation (6) but to use a filter that is as close as possible to a Fourier cutoff. We shall see that there are other compelling reasons to use this type of filter, and thus, its use would be natural in practice.

In order, to illustrate the explicit filtering procedure further, consider an Euler time stepping method applied to the LES equations

$$\bar{u}_i^{n+1} = \bar{u}_i^n + \Delta t \left[-\frac{\partial \bar{u}_i \bar{u}_j}{\partial x_j} - \frac{\partial \bar{p}}{\partial x_i} - \frac{\partial \tau'_{ij}}{\partial x_j} + \frac{1}{Re} \frac{\partial^2 \bar{u}_i}{\partial x_j \partial x_j} \right]^n. \quad (7)$$

Note, that the frequency content of each term on the right-hand side is limited to the bar level (provided the subgrid-scale model is properly constructed). Thus, in advancing from time level n to $n+1$ the frequency content of the solution is not altered. This fact implies that the additional filtering of the nonlinear term (plus and analogous treatment of the subgrid-scale model) is sufficient to achieve an explicit filtering of the velocity field for all time. It is also important to note that the procedure outlined above is in general different from the 'filtering of the velocity field after each time step' procedure that has appeared occasionally in the literature, i.e.,

$$\begin{aligned} \bar{u}_i^{*n+1} &= \bar{u}_i^n + \Delta t \left[-\frac{\partial \bar{u}_i \bar{u}_j}{\partial x_j} - \frac{\partial \bar{p}}{\partial x_i} - \frac{\partial \tau_{ij}}{\partial x_j} + \frac{1}{Re} \frac{\partial^2 \bar{u}_i}{\partial x_j \partial x_j} \right]^n, \\ \bar{u}_i^{n+1} &= \overline{\bar{u}_i^{*n+1}}. \end{aligned}$$

While this approach results in the correct treatment for the nonlinear term it is incorrect since the remaining terms are filtered twice. In particular, the additional filtering of the solution at the previous time level, \bar{u}_i^n is particularly harmful since the cumulative effect over several time steps implies multiple filterings of the velocity field, i.e.,

$$\bar{u}_i^{n+1} = \overline{\bar{u}_i^{n-1}} + \Delta t \overline{\bar{R}^{n-1}} + \Delta t \bar{R}^n.$$

In general, repeated application of the same filter implies a filter with increased width, and thus the procedure of filtering the velocity field after each time step results in a severe loss in spectral information.²

With the correct explicit filtering procedure established (i.e., equation (7)), we are now in a position to address some of the more subtle issues involved, the first of which is commutivity. As discussed above, the issue of commutation between the filter and derivative operators arises mainly in deriving the LES equations from the Navier-Stokes system. Explicit filtering, on the other hand, involves the decomposition of equation (6) where the filtered product, $\overline{u_i u_j}$ is replaced with $\overline{u_i u_j} + \tau'_{ij}$. As we have seen, this decomposition is not unique and the decision to add the second bar to the nonlinear term is not required in the basic derivation of the LES system but rather is used simply as a convenient means to control the frequency content of the solution. Furthermore, equation (6) is a substitution for $\overline{u_i u_j}$, which appears inside the divergence operator. Thus, perhaps surprisingly, there does not appear to be any direct commutation requirement on the second filter. Of course, there is an indirect requirement if one requires the first and second bar filters to be identical (since the former was used in the derivation of the LES system). It is not clear whether consistency in this regard is really required in practice, however, and it appears possible to use the second alternative decomposition

$$\overline{u_i u_j} = \widetilde{\overline{u_i u_j}} + \underbrace{(\overline{u_i u_j} - \widetilde{\overline{u_i u_j}})}_{\tau''_{ij}}, \quad (8)$$

where $\widehat{(\cdot)} \simeq (\cdot)$ is a (perhaps noncommuting) approximation to the primary filter.³

A second subtle issue concerning explicit filtering has to do with an associated false dissipation. The nonlinear term in the classical LES decomposition (equation (3)) is energy conserving since $\overline{u_i} \frac{d(\overline{u_i u_j})}{dx_j} = \frac{d(\overline{u_j} (1/2) \overline{u_i u_i})}{dx_j}$, and thus, an integral over the volume collapses to the surface fluxes via Gauss' theorem. Unfortunately, this situation is changed when an explicit filter is applied to the nonlinear term. The second filter on the nonlinear product prohibits the redistribution of velocity components used to obtain a divergence form and one is left with $\overline{u_i} \frac{d(\overline{u_i u_j})}{dx_j} = \frac{d(\overline{u_i u_i u_j})}{dx_j} - (\frac{d\overline{u_i}}{dx_j}) \overline{u_i u_j}$. The second term on the right-hand side does not vanish in general when integrated over the volume and in fact bears some resemblance to the turbulent production. More quantitative information regarding the false dissipation can be obtained by looking at the Fourier-space energy equation for isotropic turbulence which reads

$$\frac{dE(k)}{dt} = \overbrace{\left\langle -i \hat{u}_i^* P_i G(k) k_j \sum_{\substack{p \\ k=p+q}} \sum_q \hat{u}_i(p) \hat{u}_j(q) \right\rangle}^{T(k)} - \frac{2}{R_e} k^2 E(k),$$

where $E(k) = 1/2 \langle \hat{u}_i^* \hat{u}_i \rangle$ is the spectral energy density, \hat{u}_i is the Fourier transform of the velocity (bar omitted for simplicity), P_i is the divergence-free projection operator, $G(k)$ is the transfer function associated with the explicit filter, $(\cdot)^*$ denotes complex conjugate and $\langle \cdot \rangle$ is a shell average. It is clear, that the explicit filter affects only the nonlinear transfer term, $T(k)$. This term will be conservative if its integral vanishes, i.e., $\int_0^\infty T(k) dk = 0$. It can be shown, that the integral will indeed vanish if the filter function $G(k)$ is a Fourier cutoff that passes frequencies up to some limit k_{\max} , and if the velocity field is truncated at this level before the transfer term is

²It is important to note that the above argument does not apply to the Fourier cutoff filter where repeated application has no cumulative effect. In this special case, filtering the velocity field at each time step is permissible and is equivalent to the general procedure listed in equation (7).

³The formulation with an approximate second filter is probably always required in practice since even 'commuting' filters only do so to a specified order of accuracy.

constructed [7]. For nonsharp filters the transfer will not integrate to zero since the weighting introduced by a smoothly-varying $G(k)$ destroys the symmetries required to achieve complete cancellation. Further analysis reveals that the residual transfer arises only out of interactions with wavenumber components where $G \neq 1$. The sign of this residual transfer is not fixed kinematically but is constrained to be negative for developed turbulence with a normal down-scale energy cascade. Thus, nonsharp filters lead to a false dissipation that is proportional to the degree to which the filter departs from a sharp-cutoff. For this reason, it is important to use filters that are close approximations to a Fourier cutoff.

It is worthwhile to note, that the approximately-commuting filters developed by [5] become increasingly better approximations to a Fourier cutoff as the communication error is reduced. Thus, use of these filters will allow for a consistent explicit filtering scheme (first and second filters the same) and will introduce only a small amount of false dissipation.

3. NUMERICAL TESTS

3.1. Numerical Method

The second-order staggered mesh scheme [8] was chosen for this work due to its popularity for contemporary LES. This scheme has a number of practical advantages including strict mass, momentum, and kinetic energy conservation, properly coupled pressure and velocity fields, ease of implementation, and straightforward extension to generalized coordinate systems.

On the other hand, the scheme is of low accuracy, and thus, contaminates a broad region of the spectrum with numerical error. This latter feature actually makes the scheme well suited for this work since one can expect visible differences in the computed results when a portion of the numerical error is removed.

3.2. High Reynolds Number Channel Flow Test Case

The test case for this study is turbulent channel flow at a Reynolds number of 47100 based on centerline velocity and channel half-width (a friction velocity Reynolds number of 2000). This particular Reynolds number was chosen due to the availability of pseudo-spectral results [9] that are used as a basis for comparison. Piomelli [9] used a computational domain of height 2δ , length $(5\pi/2)\delta$ and width $(\pi/2)\delta$. Fourier expansions were used in the homogeneous direction whereas a Chebyshev expansion was used in the normal direction. The advective terms were cast in skew-symmetric form and no explicit dealiasing was performed. Sixty-four Fourier modes were used in the streamwise direction, 80 were used in the spanwise direction, and 80 Chebyshev modes were used in the normal direction.

The finite-difference mesh is identical to that used in the pseudo-spectral simulation with the exception of the distribution of points in the normal direction. The pseudo-spectral simulation uses a cosine mapping function to distribute the collocation points in the normal direction. While this distribution is necessary in order to make use of the fast Fourier transform, it leads to a mesh that is strongly stretched in the near-wall region. Experience with this type of mesh for finite-difference calculations indicates that the grid spacing becomes too coarse within a short distance from the wall. In order, to avoid this problem, the standard hyperbolic tangent mapping is used. The hyperbolic tangent mesh is designed so that the spacing of the first mesh cell away from the wall as well as the spacing at the channel centerline are very close to those of the cosine mesh. It turns out, that these constraints can be met only by increasing the number of points in the normal direction from 81 to 141.

The mesh spacings in wall units are $\Delta x^+ = 250$, $\Delta y_{\min}^+ = 1.6$, $\Delta y_{\max}^+ = 150$, and $\Delta z^+ = 40$. In terms of channel half-heights, the mesh spacings are $\Delta x/\delta = 0.12$, $\Delta y_{\min}/\delta = 8 \times 10^{-4}$, $\Delta y_{\max}/\delta = 0.075$, and $\Delta z/\delta = 0.02$.

Both the spectral and finite-difference simulations make use of the dynamic subgrid-scale model [1] with both test filtering and averaging of the equations for the model coefficient performed in planes parallel to the wall. The ratio of the test filter to LES filter is fixed at 2 in all simulations. In cases where an explicit LES filter is used, the test filter is simply adjusted to be twice as wide as the LES filter. The test filter operation is applied in physical space and the stencil width is varied to accommodate filters of various widths.

The simulations are performed with a fixed mean pressure gradient. The mass flow is not constrained, and therefore, will differ from simulation to simulation.

3.3. Explicit Filtering Strategy

Explicit filtering is restricted to the streamwise and spanwise directions. Several factors dictate this choice. Foremost of these is the desire to experiment with filter width ratios of up to 3 at a manageable cost. By expanding the mesh in only two directions, it is possible to use a filter width ratio of 3 by increasing the number of mesh points by a factor of 9. A factor of 27 is required for 3-D filtering and the cost of doing this was prohibitive. Further justification for filtering only in 2-D lies in the fact that, except for the core region, the wall-normal mesh is substantially finer than the other two directions. The turbulence is therefore resolved best in the wall-normal direction and it may be expected that the effect of explicit filtering would be seen more readily in the other two directions. Indeed, in a related study [10], it was found that refining the wall-normal mesh while leaving the other two directions unchanged resulted in very little improvement in the computed statistics. The same experiment applied to the other two directions, however, lead to a marked improvement in the results.

A sharp spectral cutoff is used for the explicit filter. This choice is dictated by the desire to respect Galilean invariance and to maintain kinetic energy conservation. The filtering itself is implemented via with fast Fourier transforms with an associated direct numerical overhead of 10%.

3.4. Results from the Explicitly Filtered Simulations

Simulations were run with filter width ratios of 1.0, 1.5, and 3.0 (refer to Table 1). The mesh was enlarged in the streamwise and spanwise directions by a factor equal to the filter width ratio in each case so that the effective resolution was constant. The modified wavenumber diagram for these simulations are shown in Figure 1. The chain-dashed vertical line denotes the fixed-effective resolution, while the solid curves to the left of this line show the modified wavenumber distributions for the various levels of filtering. When no filter is applied (lowest solid curve in Figure 1) considerable truncation error is evident for the upper half of the wavenumber range. As the filter width ratio is increased, the situation improves. The error might seem to be acceptable for a filter width ratio of 3.

Figure 2 shows a comparison of the mean velocity profiles from the explicitly filtered simulations, plotted in wall coordinates. The pseudo-spectral results of [9] are also included for reference. Starting with the unfiltered simulation, it is seen that the velocity profile deviates strongly from the accepted log-law. Although a logarithmic region is present, the slope is too low and intercept is overpredicted by more than 100%. The mass flow is also overpredicted by 6.3% compared with the correlations of Dean [11].

A comparison of the unfiltered case with the pseudo-spectral simulation provides some insight regarding the role of truncation errors when the second-order scheme is used for high Reynolds number LES. From Figure 2 it is clear that the second-order scheme is not able to reproduce even the lowest-order statistics when compared with a pseudo-spectral simulation at the same resolution. Although this might be expected, it is in contrast to the findings of Choi *et al.* [12] who obtained a good match with pseudo-spectral results when applying the same finite-difference scheme to low Reynolds number direct numerical simulations (DNS) of channel flow. The shift

Table 1. Mesh and effective resolution for the various simulations.

Case	Mesh			Filter Ratio	Effective Resolution		
	N_x	N_y	N_z		N_x	N_y	N_z
A	64	141	80	1.0	64	141	80
B	96	141	120	1.5	64	141	80
C	192	141	240	3.0	64	141	80
D	96	141	120	1.0	96	141	120
E	192	141	240	1.0	192	141	240

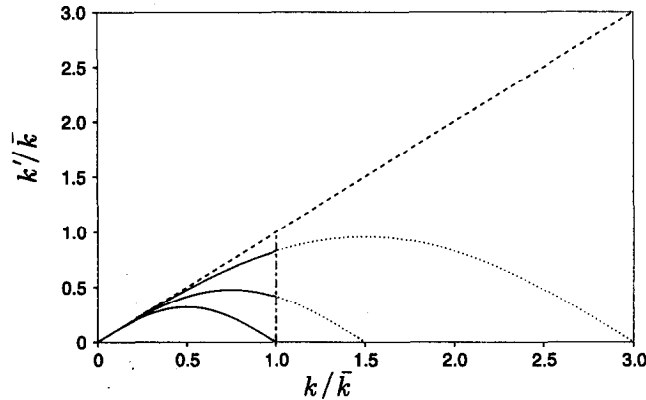


Figure 1. Modified wavenumber diagram for the various simulations. From bottom to top the solid lines are for filtered simulations using filter width ratios of 1.0, 1.5, and 3.0, respectively. The vertical chain-dashed line represents the effective resolution of the filtered simulations which was held fixed by expanding the mesh by factor equal to the filter width ratio in each case. From bottom to top, the dotted curves show the modified wavenumber distributions for the unfiltered simulations performed on the meshes expanded by factors of 1.5 and 3.0, respectively. The dashed line is the exact distribution that is achieved with a pseudo-spectral method.

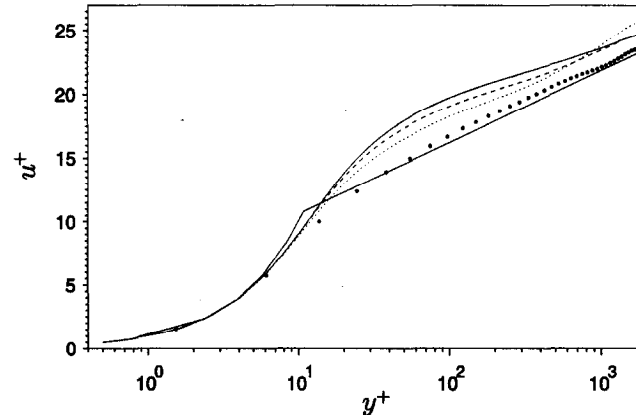


Figure 2. Mean velocity profiles from the explicitly filtered simulations. — filter width ratio 1.0; - - - 1.5; . . . 3.0; • pseudo-spectral results of [9]. The viscous sublayer ($u^+ = y^+$) and log-law ($u^+ = 2.44 \ln(y^+) + 5.0$) solutions are also shown for reference.

in behavior in the present results is almost certainly due to the relative increase in numerical error in the LES resulting from the substantial increase in energy in the smallest resolved length scales. The relatively good performance of the second-order scheme in the DNS of [12] was probably aided further by the fact that the DNS was very well resolved. Kim *et al.* [13] reported no significant change of their spectral DNS results when they coarsened the resolution in the streamwise and spanwise directions by approximately 30%.

Returning to the curves in Figure 2, it is clear, that filtering improves the mean velocity profile. In particular, the log-law intercept decreases toward the usual value and the slope improves. A noticeable wake develops in the outer region of the velocity profile for the case with a filter width ratio of 3. This wake is somewhat larger than the one observed in the pseudo-spectral results, but is similar to those observed in experimental data.

Although explicit filtering clearly improves the mean velocity profile, the rate of convergence to the pseudo-spectral results appears to be rather slow. Significant errors still exist for a filter width ratio of 3 and a simple extrapolation of these results would seem to indicate that a filter width ratio as large as 6 would be required to recover the standard log-law.

Figure 3 shows the velocity fluctuation profiles plotted in wall coordinates. Starting with the unfiltered case, it is apparent that the second-order scheme is unable to reproduce the pseudo-spectral results at high Reynolds number. The streamwise fluctuation is overpredicted and the other two components are underpredicted. This exaggerated near-wall anisotropy is characteristic of the second-order scheme when the mesh is too coarse. When explicit filtering is used, the results are seen to improve. The streamwise velocity fluctuation is reduced and the anisotropy is improved. Once again, the rate of convergence to the pseudo-spectral results is slow it appears that a filter width ratio in excess of 3 is required to recover spectral-like accuracy.

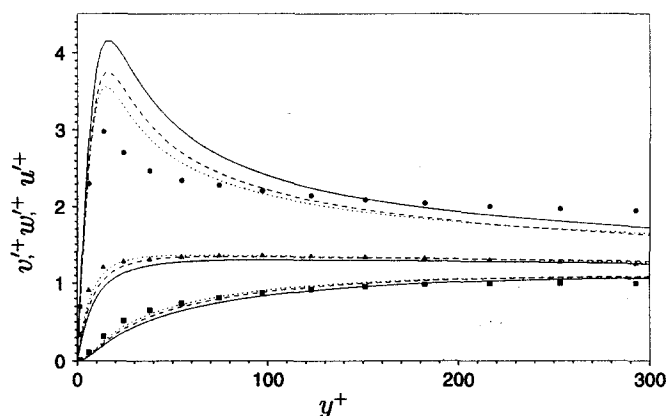


Figure 3. Velocity fluctuation profiles from the explicitly filtered simulations. — filter width ratio 1.0; --- 1.5; ... 3.0; •, ■, and △ u'^+ , v'^+ , and w'^+ from the pseudo-spectral calculation of [9].

As discussed in the introduction, explicit filtering can improve the dynamic model calculation of the subgrid-scale model constant since the scales that it samples will be better resolved. This effect is demonstrated in Figure 4a where the subgrid-scale shear stress is plotted in the near-wall region. When no explicit filter is used, the subgrid-scale shear stress is underpredicted by about a factor of 2 when compared with the value from the pseudo-spectral simulation. Although it cannot be seen from Figure 4a, the stress is too low over the entire channel. Filtering improves this situation by increasing the stress level throughout the channel. When a filter width ratio of 3 is used, the stress is still about 20% low at the maximum, but is very close to the pseudo-spectral prediction over much of the rest of the channel.

One interesting feature of the subgrid-scale shear stress distributions is the discrepancy in the location of the maximum value between the finite-difference and pseudo-spectral calculations. The peak value from the pseudo-spectral simulation is at roughly 12 wall units, whereas a maximum does not occur until about 30 wall units in the finite-difference simulation. The position of the maximum in the finite-difference simulation is insensitive to filter width ratio which seems to indicate that the discrepancy is not a result of truncation error from the streamwise or spanwise directions. The discrepancy could result from wall-normal truncation error in the finite-difference calculation although this would seem unlikely given the very fine mesh in the near-wall region.

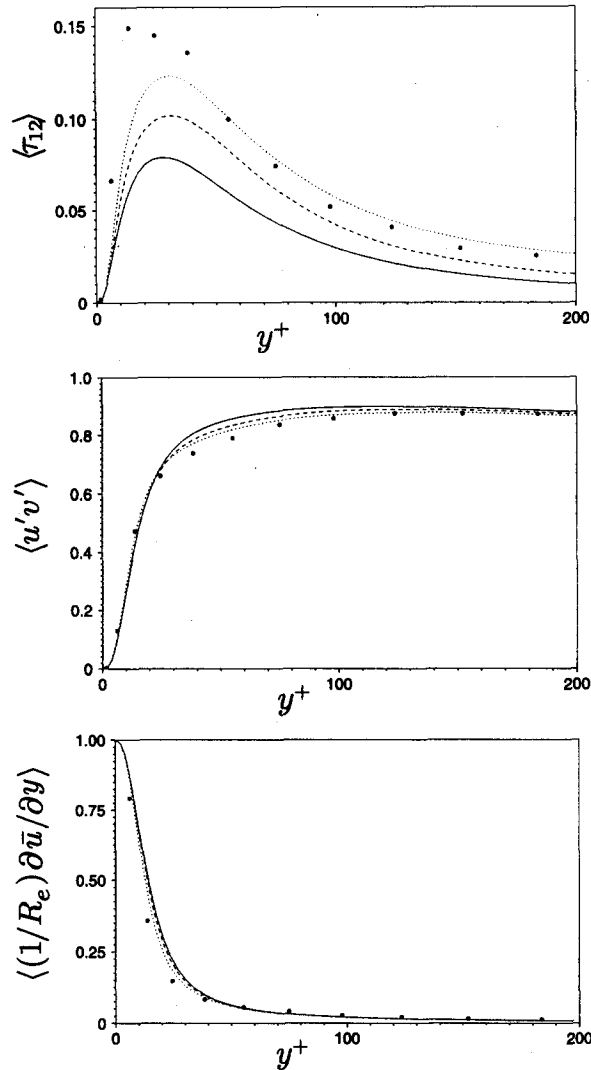


Figure 4. Shear stress profiles from the explicitly filtered simulations. (a) subgrid-scale shear stress, (b) resolved shear stress, (c) viscous shear stress. In each case — filter width ratio 1.0; — — 1.5; ··· 3.0; • pseudo-spectral results of [9].

At the same time, the collocation points near the wall are much more coarsely spaced in the pseudo-spectral simulation and this may affect the prediction of the stress maximum.

The resolved and viscous shear stress profiles are shown in Figures 4b and 4c. Both these stress components are generally over-predicted when no explicit filter is used. The results improve when the simulation is filtered, and the stresses from the case using a filter width ratio of 3 are in reasonable agreement with the pseudo-spectral results.

3.5. Results from Mesh Refinement without Explicit Filtering

As discussed in the introduction, it is of interest to compare the effectiveness of explicit filtering against straightforward mesh refinement. The explicitly filtered simulations make use of a fine mesh, but discard the high-frequency, error-prone scales. Simulations performed on the same fine mesh but without explicit filtering cost roughly the same but include a broader range of motions. The smallest of these are certainly polluted by numerical error, but they may be far enough removed from the energy-containing scales that the errors do not significantly effect the low-order statistics.

The tradeoff between explicit filtering and straightforward mesh refinement was studied by performing two additional simulations on the same meshes used in the explicit filter study, but without application of the filter. The parameter for these simulations are summarized in Table 1 and the corresponding modified wavenumber diagrams are shown in Figure 1.

Note, that the modified wavenumber distributions for the refined simulations are identical to the filtered cases up to the cutoff wavenumber. Thus, this portion of the spectrum is subject to the same numerical errors in both the filtered and refined cases. The difference between the two series is that the refined simulations include the motions intermediate between the LES filter and the mesh resolution limit. The additional scales are subject to considerable numerical error, but these errors are concentrated at increasing wavenumber as the level of refinement is increased. In particular, note that when the mesh is refined by a factor of 3, the modified wavenumber does not begin to decrease until 1.5 times the cutoff wavenumber (for the filtered simulations). The error increases appreciably only after this point and it is plausible that the useful resolution of this simulation is roughly 50% higher than in the corresponding filtered case.

Figure 5 shows a comparison of the mean velocity profile from the simulations with mesh refinement. The most noticeable change is a decrease in the mean velocity for the fixed-wall shear as the mesh is refined. The quality of the logarithmic region is essentially unchanged however, and its extent decreases with increasing resolution. If a straight line is fit through the "logarithmic" region, the log law intercept is found to improve as the resolution is increased and is roughly correct for a factor of 3 mesh refinement. The slope of the "logarithmic" region does not improve with mesh refinement, however, and the profile for the factor of 3 refinement displays an unusual oscillation about the expected logarithmic distribution. In comparing the profiles from the filtered and unfiltered simulations performed on the same mesh (Figures 2 and 5) it is clear that the log-law intercept is better predicted by the refined simulations without filtering, whereas the slope and extent of the log region is better predicted when the simulation is filtered. Thus, it appears that a rough prediction of the correct profile shape can be achieved more efficiently via mesh refinement, whereas the finer details of the velocity distribution may require the removal of at least some of the numerical error. It is also interesting to note, that the profiles from the filtered simulations (Figure 2) have evidently not saturated due to numerical error arising from the wall-normal direction. Figure 5 for the unfiltered simulations shows that it is possible to achieve roughly the correct log-law intercept without improving the wall-normal resolution. Thus, it might be expected that the filtered simulation profiles shown in Figure 2 would continue to improve if the filter width ratio were increased further.

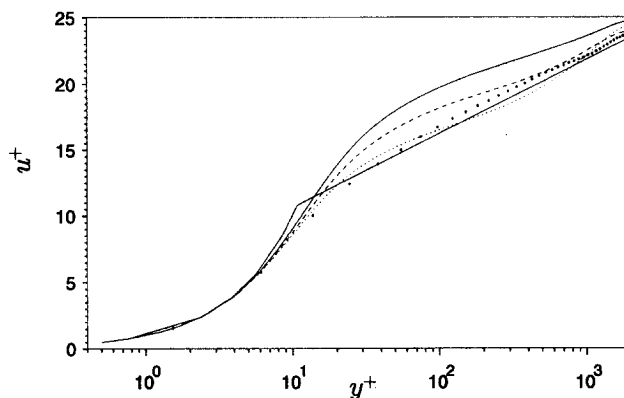


Figure 5. Mean velocity profiles from the refined simulations. — no refinement; --- 1.5 increase in resolution; ... 3.0 times increase in resolution; • pseudo-spectral results of [9]. The viscous sublayer ($u^+ = y^+$) and log-law ($u^+ = 2.44 \ln(y^+) + 5.0$) solutions are also shown for reference.

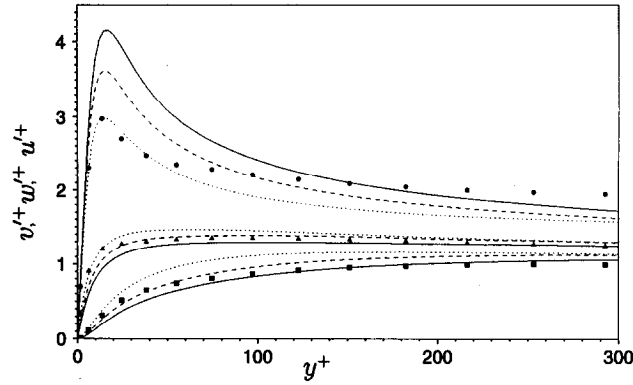


Figure 6. Velocity fluctuation profiles from the refined simulations. — no refinement; --- 1.5 times increase in resolution; ... 3.0 times increase in resolution, •, ■, and △, u'^+ , v'^+ , and w'^+ from the pseudo-spectral calculation of [9].

Velocity fluctuation profiles from the mesh refinement series are shown in Figure 6. The velocity fluctuations are seen to respond strongly to increased resolution with the streamwise component showing the greatest improvement. For a factor of 3 increase in resolution, the streamwise velocity fluctuation agrees very well with the pseudo-spectral results in the vicinity of the maximum but appears to be somewhat low as the distance from the wall is increased. Both the wall-normal and spanwise velocity fluctuations increase in the near-wall region as the mesh is refined and appear to exceed the values from the pseudo-spectral simulation. Part of this effect is due to increased variance coming from the additional small-scale motions supported by the refined meshes in the finite-difference simulations. In order, to make an exact comparison, the finite-difference data in Figure 6 should really have been filtered back to the resolution of the pseudo-spectral simulation as the statistics were accumulated. Such a filtering of the statistics might also lower the streamwise fluctuation, and could affect the apparent agreement with the pseudo-spectral results.

In comparing the filtered and unfiltered simulations run on the same mesh (Figures 3 and 6) it is again apparent that the statistics improve faster when the mesh is simply refined. Unlike the mean velocity profile, however, there do not appear to be any anomalous features associated with the velocity fluctuations when the numerical error is not removed from the simulation.

4. CONCLUSIONS

A general framework for explicit filtering in LES has been presented and several subtle features of this implementation have been pointed out. In particular, the explicit filter should be a close approximation to a Fourier cutoff in order to minimize Galilean invariance error and to minimize false dissipation.

Results of turbulent channel flow simulations established the fact that explicit filtering can improve the accuracy of LES performed with a second-order accurate finite-difference scheme. In particular, the quality of the logarithmic region of the mean velocity profile for turbulent channel flow is improved as is the near-wall anisotropy of the velocity fluctuations. The dynamic subgrid-scale model estimation of the shear stress component is also improved. While the computed statistics clearly improve with explicit filtering, the rate of convergence is rather slow. Even a filter width ratio of 3 is evidently insufficient to produce results that compare well with a pseudo-spectral simulation at the same effective resolution.

Mesh refinement without explicit filtering was found to improve the statistics at a greater rate when compared with the filtered simulations. This result seems to indicate that there is some benefit from including additional smaller scales in the simulations even if they are contaminated by numerical error. This is probably due to the fact that the error is pushed out to higher

wavenumber where it has a relatively weak impact on the low-order statistics. Signs of the residual error are evident in the mean velocity profile, however, and it may not be possible to obtain highly accurate statistics without at least some level of numerical error removal.

The basic message from both the explicit filtering and mesh refinement simulations is that, while the results are clearly improved when numerical error is reduced, the cost of doing so via either mechanism is considerable. Although a factor of 3 refinement of the mesh gives acceptable agreement with pseudo-spectral simulation results, this represents a factor of 27 increase in cost for a simulation that is refined in all three directions. Even in the present case of two-dimensional refinement, the cost is increased by nearly an order of magnitude. It is possible that a slight gain may be realized by combining some level of mesh refinement and explicit filtering. For example, it is possible that even better results could be obtained using a mesh that is expanded by a factor of three and then filtered using a filter width ratio 1.5 so, that the effective resolution is doubled. It is doubtful that this strategy would lead to a significant reduction in cost, however.

The results of the present study also hint that a higher-order scheme may be a more cost-effective means at achieving acceptable accuracy. For example, the relative truncation error in a fourth-order scheme can be reduced by the same amount as in the second-order simulation using a mesh expanded by a factor of 1.7 as opposed to a factor of 3. By the same token, the use of an explicit filter may be more effective at moderate filter width ratios when applied to a fourth-order scheme.

REFERENCES

1. M. Germano, U. Piomelli, P. Moin and W.H. Cabot, A dynamic subgrid-scale eddy viscosity model, *Phys. Fluids A* **3**, 1760–1765 (1991).
2. S. Ghosal, T.S. Lund, P. Moin and K. Akselvoll, A dynamic localization model for large-eddy simulation of turbulent flows, *J. Fluid. Mech.* **286**, 229–255 (1995).
3. S. Ghosal and P. Moin, The basic equations of the large eddy simulation of turbulent flows in complex geometry, *J. Comp. Phys.* **118**, 24 (1995).
4. H. van der Ven, A family of large eddy simulation (LES) filters with nonuniform filter widths, *Phys. Fluids* **7**, 1171 (1995).
5. O. Vasilyev, T.S. Lund and P. Moin, A general class of commutative filters for LES in complex geometries, *J. Comp. Phys.* **146**, 82–104 (1998).
6. R.S. Rogallo and P. Moin, Numerical simulation of turbulent flow, *Ann. Rev. Fluid Mech.* **16**, 99 (1984).
7. R.H. Kraichnan, Eddy viscosity in two and three dimension, *J. Atmos. Sci.* **33**, 1521–1536 (1976).
8. F.H. Harlow and J.E. Welch, Numerical calculation of time-dependent viscous incompressible flow of fluid with a free surface, *Phys. Fluids* **8**, 2182–2189 (1965).
9. U. Piomelli, High Reynolds number calculations using the dynamic subgrid-scale stress model, *Phys. Fluids A* **5**, 1484–1490 (1993).
10. T.S. Lund, H.-J. Kaltenbach and K. Akselvoll, On the behavior of centered finite difference schemes for large eddy simulation, *Proceedings of the Sixth International Symposium on Computational Fluid Dynamics*, Lake Tahoe, NV (1995).
11. R.B. Dean, Reynolds number dependence of skin friction and other bulk flow variables in two-dimensional rectangular duct flow, *Trans. ASME I: J. Fluids Engng.* **100**, 215 (1978).
12. H. Choi, P. Moin and J. Kim, Turbulent drag reduction: Studies of feedback control and flow over riblets, Rep. TF-55, Thermosciences Div., Dept. Mech. Eng., Stanford University, Stanford, CA (1992).
13. K. Kim, P. Moin and R. Moser, Turbulent statistics in fully developed channel flow at low Reynolds number, *J. Fluid. Mech.* **177**, 133–166 (1987).